RESEARCH ARTICLE

Clinical Manifestations and Imaging Characteristics of Gliomatosis Cerebri with Pathological Confirmation

Chun-Pu Zhang[1], Hua-Qing Li[2], Wei-Tao Zhang[3], Ming-Hui Liu[4]*, Wen-Jing Pan[2]

Abstract

Objective: To explore the clinical manifestations and imaging characteristics of gliomatosis cerebri to raise the awareness and improve its diagnostic accuracy for patients. Materials and Methods: Clinical data, imaging characteristics and pathological examination of 12 patients with GC from Jan., 2008 to Jan., 2012 were analyzed retrospectively. Results: Patients with GC were clinically manifested with headache, vomiting, repeated seizures, fatigue and unstable walking, most of whom had more than 2 lesions involving in parietal lobe, followed by temporal lobe, frontal lobe, periventricular white matter and corpus callosum. Magnetic resonance imaging (MRI) showed diffuse distribution, T1-weighted images (T1WI) with equal and low signals and T2-weighted images (T2WI) with bilateral symmetrical high diffuse signals. There was no reinforcement by enhancement scanning and signals were different in diffusion-weighted images (DWI). The higher the tumor staging, the stronger the signals. Pathological examination showed neuroastrocytoma in which tumor tissues were manifested by infiltrative growth in blood vessels and around neurons. Conclusions: In clinical diagnosis of GC, much attention should be paid to the diffuse distribution of imaging characteristics, incomplete matching between clinical and imaging characteristics and confirmation by combining with histopathological examination.

Keywords: Gliomatosis cerebri - clinical manifestation - imaging characteristics - pathological examination

Asian Pac J Cancer Prev, **15 (11)**, 4487-4491

Introduction

Gliomatosis cerebri (GC) is a rare primary tumor of central nervous system (CNS), pathologically marked by diffuse invasive hyperplasia, but capable of keeping the completeness of anatomical structure. According to the classification of nervous system neoplasms made by World Health Organization (WHO) (Rees et al., 2011), GC can be classified as astrocytic tumor of neuroepithelial tissue tumors with high-degree malignancy, mostly involving three or more lobes and bilateral hemicerebrum, and extending to infratentorial structure and even spinal cord. It is difficult to diagnose GC because of the diversification in clinical manifestation and the absence of specificity of imaging examination. Therefore, this study retrospectively analyzed the clinical manifestations and imaging and pathological characteristics in 12 patients with GC, whose results were reported as follows.

Materials and Methods

General data

A total of 12 patients with GC in Department of Neurology, Affiliated Hospital of Taishan Medical University from Jan., 2008 to Jan., 2012 were selected, in which there were 7 males and 5 females, aging from 18 to 56 years, with average age of (29.4±6.3) years. The course of disease was 3 months to 2 years with the average being (9.5±4.7) months. The clinical manifestations of GC were mainly headache, vomiting, epilepsy, slurred speech and mental abnormality. Before hospitalization, 3 patients were diagnosed with encephalitis, 2 with cerebral infarction, 2 with metabolic encephalopathy, 1 with demyelinating diseases and 4 with intracranial mass of unknown origin.

Methods

The clinical manifestations of 12 patients were observed. All patients were followed up for 6~30 months and the survival time was recorded.

Laboratory examination: Ten patients were performed with lumbar puncture to detect protein content in intracranial pressure (ICP) and cerebrospinal fluid (CSF). Imaging examination: Eight patients were performed with routine head CT scan, scanning range from orbitomental line (OML, base line) to the top of the head in routine recumbent position 24 h after hospitalization. CT examination adopted SOMATOM Emotion16 from Germany's Siemens, 120 KV, 250 mA, 2 s scanning, 5 mm in thickness and 5 mm in pitch. All patients were given

*[1]Department of Neurosurgery, [2]ICU, Affiliated Hospital of Taishan Medical University, [3]Department of Otolaryngology, [4]Specialist Ward, Central Hospital, Shangdong Energy Feicheng Mining Group Co. Ltd, Tai'an, China *For correspondence: Lmh09910991@126.com*

Table 1. Clinical Manifestations of 12 Patients with GC

No.	Clinical manifestation	Location of lesions	Pathological diagnosis	Types
1	Headache, vomiting, fatigue, unstable walking, facial numbness	Bilateral temporal lobe,parietal lobe	Level I~II	Type I
2	Headache, vomiting, epilepsy, alalia	Left temporal lobe, frontal lobe, occipital lobe	Level I	Type I
3	Fatigue, unstable walking, slurred speecha, hypomnesis	Right parietal lobe, temporal lobe, frontal lobe, corpus callosum	Level II	Type II
4	Headache, vomiting, epilepsy, slurred speech, hypomnesis	Left parietal lobe, temporal lobe, bilateral frontal lobe, basal ganglia, thalamus	Level II	Type I
5	Headache, vomiting	Left parietal lobe, frontal lobe, corpus callosum	Level III	Type I
6	Epilepsy, fatigue, unstable walking	Right parietal lobe, brainstem Level I~II	Type II	
7	Headache, vomiting, slurred speech, facial numbness	Bilateral frontal lobe, left basal ganglia, cerebellum	Level II	Type I
8	Headache, vomiting, epilepsy	Left parietal lobe, temporal lobe, occipital lobe, bilateral frontal lobe	Level II	Type II
9	Headache, vomiting, fatigue, unstable walking	Right parietal lobe, temporal lobe, corpus callosum, brainstemcerebellum	Level II	Type II
10	Epilepsy, slurred speech, disturbance of consciousness	Bilateral parietal lobe, frontal lobe, left thalamus	Level II	Type I
11	Epilepsy, fatigue, unstable walking	Left parietal lobe, temporal lobe, occipital lobe, bilateral basal ganglia	Level III	Type I
12	Headache, vomiting, fatigue, unstable walking	Right parietal lobe, temporal lobe, corpus callosum, brainstem	Level II	Type I

MRI plain scan and enhancement scan. MRI examination employed Philips gyroscan intera 0.5T MR with spin-echo T1-weighted image (T1WI), T2-weighted image (T2WI) and fluid-attenuated inversion-recovery sequence (FLAIR) in transverse view, and T1WI and T2WI image were 6~8 mm in thickness in sagittal view. GD-DTPA (0.1 mmol/kg) was used as contrast agent for enhancement scan and T1WI scanning after intravenous injection. 10 cases were performed with diffuse weighted image (DWI), and 8 with magnetic resonance spectroscopy (MRS). According to the presence of local mass detected by imageological examination, 12 patients were divided into 2 types: type I had no mass while type II had 1~2 masses with enhancement effect (Cai et al., 2011).

Pathological examination: Twelve patients were conducted with MRI-guided stereotactic biopsy. After sample fixation, HE staining and GFAP staining were done.

Statistical data analysis

SPSS 15.0 software was used for statistical analysis. Measurement data was expressed by ($\chi\pm s$) and t test was employed for comparisons among groups. $P<0.05$ was considered to be statistically significant.

Results

Clinical manifestation and follow-up results

Of the 12 patients with GC, 8 (66.7%) were clinically manifested with increased intracranial pressure such as headache and vomiting, 6 (50%) with repeated seizures, another 6 (50.0%) with fatigue and unstable walking, 5 (41.7%) with slurred speech, 3 with hypophrenia and mental abnormality and 2 (16.7%) with facial numbness (Table 1). Follow-up till April, 2014, and patients were all dead with mean survival time (MST) being (10.5±6.3) months. There were 3 patients in level I or level I~II with the MST being (18.2±2.8) months, 7 in level II with the MST being (11.3±3.9) months, and 2 in level III with the MST being (3.5±0.9) months. Through statistical analysis, there were significant differences among level I or level I~II and level II ~III ($P<0.05$ or $P<0.01$) and there was significant difference between level II and level III ($P<0.05$).

Laboratory results

Of 10 patients with lumber puncture, 8 were with increased CSF pressure by 258 mm H2O in average and 3 with increased protein content by 640 mg/L, 657 mg/L, and 669 mg/L, respectively.

Imaging examination results

CT examination results: Of 8 patients performed with head CT scan, 2 had no abnormal changes and the lesion was mainly located in the brainstem under MRI examination. For the other 6 patients, there were 4 with slightly low-density diffuse patchy abnormal signal and 2 with slightly high-density diffuse patchy abnormal signal, mainly involving in temporal and frontal lobes, 5 with perifocal pitting edema and 3 with apparent intracranial mass but without reinforcement in lesions.

MRI examination results: The lesions of all patients had multiple involved parts, in which 2 patients with 2 parts, 3 with 3 parts, 7 with 4 parts or more. There were 4 patients involving in unilateral parts and corpus callosum, 2 in unilateral parts and 6 in bilateral parts. Parietal lobe (10 cases) topped the list of lesion sites, followed by temporal lobe (8 cases), frontal lobe (7 cases), periventricular white matter and corpus callosum (4 cases), occipital lobe (3 cases), basal gangalia (3 cases), thalamus (2 cases), brainstem and (1 case) (Table 1). Imaging characteristics of MRI were mainly manifested bydiffuse distribution in lesions without cystoid variation, calcification and obvious necrosis. T1WI showed equal and low signal while T2WI showed bilateral symmetrical diffuse high signal and significant high signal in FLAIR. All patients were examined

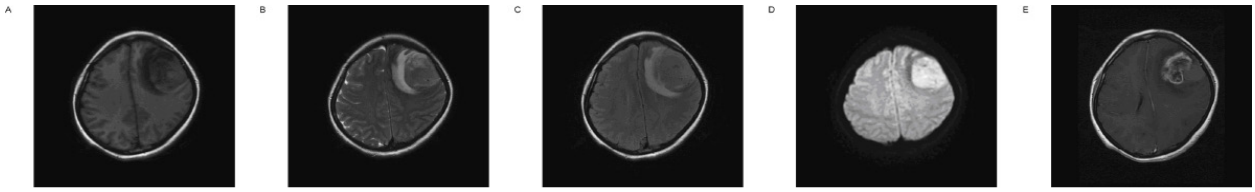

Figure 1. MRI mainly showed the shadow of mixed signals in equal T1, in which slightly long cystic T2 signal shadow was seen (**A, B and C**). DWI showed slightly high signal (**D**). Long T1 and long T2 edema signals were seen in lesions. By enhancement scanning, the edge of lesions showed obvious ring reinforcement and medium reinforcement shadow around the lesion (**E**). There was no obvious reinforcement in surrounding meninges and edema areas. Left lateral ventricle was under pressure, midline shifting to the right

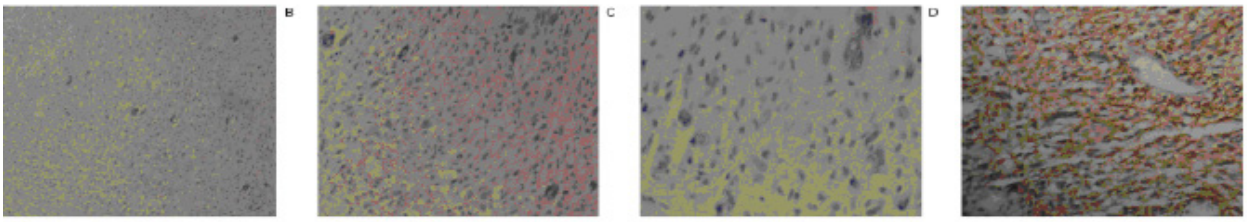

Figure 2. Under the Macroscope, Glioma Cells Mainly Showed Diffuse Infiltrating Astrocyte with Small Body and Polymorphism (mainly fusiformis or roundness), Nuclear Hyperchromatism and a Few of Nuclear Division. A. HE staining ×100; HE staining ×200; C. HE staining ×400; D. GFAP staining ×400

with enhancement scan, in which 8 had no obvious reinforcement, 2 with pitchy reinforcement and the other 2 with perifocal patchy reinforcement. In 10 patients with DWI, the signals were different, and the higher the tumor stage was, the stronger the signal was (Figure 1). MRS analysis showed that ratios of Cho/Cr and Cho/NAA both increased in tumor parenchyma.

Pathological examination results: The pathological examination results of all 12 patients showed neuroastrocytoma, the tumor tissues of which were manifested by infiltrative growth in blood vessels and around neurons, . HE staining showed cell nucleus heteromorphism and nuclear division in different degrees without obvious necrosis and vascular proliferation. Glioma cells by GFAP staining presented positive expression (Figure 2). The levels of tumor: 1 patient in level I, 2 in level I~II, 7 in level II and 2 in level III.

Discussion

High incidences of tumors of the brain and nervous system have been noted in Brazil, the US and the Hawaiian islands among the white population, Canada , Italy Poland, Finland an other European countries, and low incidence was found in Africa and Asia (Cheng et al., 2013; Igissinov et al., 2013; Jazayeri et al., 2013; Liang et al., 2013; Zeybek et al., 2013; Zhang et al., 2013). GC is a special kind of tumor of CNS, for which invasive growth is its typical biological behavior and the key factor of high reoccurrence rate and short survival time. In 1938, Nevin (Taillibert et al., 2011) first reported this disease and 296 patients with GC were reported in foreign literatures in 2006. It is difficult to diagnose GC because of its involvement in many locations, the diversification in clinical manifestation and MRI and the absence of specificity of imaging examination (Paulus et al., 2010; Landi et al., 2011).

The onset range of GC, ranging from infants of months to the elderly of 85 years, is large and there is no significant difference in morbidity between males and females (Taillibert et al., 2006; Narasimhaiah et al., 2012; Sun et al, 2012). GC is often misdiagnosed as cerebral hemorrhage disease and encephalitis in that its primary symptoms include headache, vomiting and stroke with less positive signs in initial stage, and (Rooney et al, 2013; Boele et al, 2014; Rudà et al, 2014). According to WHO Criteria in Tumor (Herrlinger et al, 2002), the severity of malignancy belong to level III manifested as diffuse lesions, often involving in 2 or more lobes and bilateral brain tissues, and extending to infratentorial structures and even to spinal cord. Additionally, GC also has high malignancy, fast progress and short survival time. Previous report showed that MST in patients with chemotherapy (10 cases) and radiotherapy combined with chemotherapy (10 cases) was longer than those with radiotherapy (5 cases), but the differences were not significant because of the little samples (Landi et al, 2011). Another study of 54 patients with cerebral flioma found that median overall survival (OS) was 18.5 months (Chen et al, 2013). In this study, all patients, with large span in age ranging from 18 to 85 years, were clinically marked by headache, vomiting, repeated seizures, fatigue, unstable walking, slurred speech, hypophrenia and mental abnormality. The patients had more than 2 lesions, mostly involving in parietal lobe, followed by temporal lobe, frontal lobe, periventricular white matter and corpus callosum. Moreover, the survival time of patients in level I and level I~II was longer than those in level II and level III, which was basically consistent with the above literatures.

As for imaging diagnosis, it is difficult for MRI to differentiate the types and levels of GC and accurately show the edges of invasive tumors. It is widely believed in clinic that tumors with richer blood supply had higher malignant degree. Therefore, MRI examination with perfusion sensitivity was considered as the golden standard in the diagnosis of GC because it contributes

to the differential diagnosis of degenerative glioma and spongioblastoma, in which T2WI is capable of showing high signal changes (Federau et al., 2014; Hu et al., 2012; Fan et al., 2006). DWI is currently the only technique of measuring living diffusion and to some extent, compensates the shortness of routine MRI (Liu et al., 2011; Liu et al., 2012; Lober et al., 2014).

In Sinha's study, patients with high levels of GC, patients with brain edema and healthy people were performed with DWI and the results indicated that the average diffusion coefficients were significantly different among groups. Numerical value of necrotic tumor center topped the list of the average diffusion coefficients, followed by brain edema, tumor reinforcement center and the reinforcement edges of tumors (Sinha et al., 2002). A comparative study of traditional MRI examination, MRI with perfusion imaging and MRS for the brain glioma grading suggested that the diagnosis sensitivity, specificity, positive/negative predictive values of high-level brain glioma by traditional MRI examination were 72.5%, 65.0%, 86.1% and 44.1%, respectively. When relative cerebral blood volume (rCBV) was 1.75, diagnosis sensitivity, specificity, positive/negative predictive value showed by MRI with perfusion imaging were 95.0%, 57.5%, 87.0% and 79.3%, respectively. Peak value and specific value of Cho, Cr and NAA observed by MRS revealed that the value of Cho/Cr was 0.69 (1.08/1.56) and that of Cho/NAA was 0.71 (0.75/1.06). The results showed that the diagnosis sensitivity, specificity, positive/negative predictive value by MRI with perfusion imaging and MRS for low-level and high-level GC were obviously higher than traditional MRI examination (Sinha et al., 2002; Law et al., 2003). In this study, the MRI characteristics were manifested with diffuse distribution in lesions involving in more than 2 parts, obvious intracranial mass in unilateral lesions, long or equal T1 signal, long T2 signal and significant changes in FLAIR.

GC has unique characteristics marked by diffuse growth of tumor cells in brain parenchyma, obscure margin, differentiated tumor cells showing astrocyte and oligoastrocytic features (Park et al., 2009; Porter et al., 2010). If there are tumor cell infiltration in cerebral cortex, satellite phenomenon surrounding neuron occurs. The type I GC can be transformed into type II and GC may be transformed into glioblastoma (Claes et al., 2007; Romeike et al., 2008). In this study, of all patients with neuroastrocytoma, 10 were with surface infiltration of brain cells and positive GFAP staining in tumor cells.

In conclusion, GC is a kind of malignant tumor with diversity in clinical manifestation, difficulty in diagnosis and absence of specific biological characteristics. In clinical diagnosis, more attention should be paid to diffuse distribution in imaging characteristics, incomplete matching between clinical and imaging characteristics and confirmation when combined with histopathological examination.

References

Boele FW, Leeuw IM, Cuijpers P, et al (2014). Internet-based guided self-help for glioma patients with depressive symptoms: design of a randomized controlled trial. *BMC Neurol*, **14**, 81.

Cheng HB, Xie C, Zhang RY, et al (2013). Xeroderma pigmentosum complementation group of polymorphisms influence risk of glioma. *Asian Pac J Cancer Prev,* **14**, 4083-7.

Claes A, Idema AJ, Wesseling P (2007). Diffuse glioma growth: a guerilla war. *Acta Neuropathol*, **114**, 443-58.

Cai L, Gao S, Li Y, et al (2011). 11C-Methionine or 11C-Choline PET is superior to MRI in the evaluation of gliomatosis cerebri. *Clin Nucl Med,* **36**, 127-9.

Chen S, Tanaka S, Giannini C, et al (2013). Gliomatosis cerebri: clinical characteristics, management, and outcomes. *J Neurooncol*, **112**, 267-5.

Federau C, Meuli R, O'Brien K, et al (2014). Perfusion Measurement in Brain Gliomas with Intravoxel Incoherent Motion MRI. *Am J Neuroradiol*, **35**, 256-62.

Fan GG, Deng QL, Wu ZH, et al (2006). Usefulness of diffusion/perfusion-weighted MRI in patients with non-enhancing supratentorial brain gliomas: a valuable tool to predict tumour grading. *Br J Radiol*, **79**, 652-8.

Herrlinger U, Felsberg J, Küker W, et al (2002). Gliomatosis cerebri: molecular pathology and clinical course. *Ann Neurol*, **52**, 390-9.

Hu LS, Eschbacher JM, Heiserman JE, et al (2012). Reevaluating the imaging definition of tumor progression: perfusion MRI quantifies recurrent glioblastoma tumor fraction, pseudoprogression, and radiation necrosis to predict survival. *Neuro Oncol*, **14**, 919-30.

Igissinov N, Akshulakov S, Igissinov S, et al (2013). Malignant tumours of the central nervous system in Kazakhstan--incidence trends from 2004-2011. *Asian Pac J Cancer Prev,* **14**, 4181-6.

Jazayeri SB, Rahimi-Movaghar V, Shokraneh F, et al (2013). Epidemiology of primary CNS tumors in Iran: a systematic review. *Asian Pac J Cancer Prev,* **14**, 3979-85.

Law M, Yang S, Wang H, et al (2003). Glioma grading: sensitivity, specificity, and predictive values of perfusion MR imaging and proton MR spectroscopic imaging compared with conventional MR imaging. *Am J Neuroradiol*, **24**, 1989-98.

Landi A, Piccirilli M, Mancarella C, et al (2011). Gliomatosis cerebri in young patients' report of three cases and review of the literature. *Child's Nervous System*, **27**, 19-25.

Liang HJ, Yan YL, Liu ZM, et al (2013). Association of XRCC3 Thr241Met polymorphisms and gliomas risk: evidence from a meta-analysis. *Asian Pac J Cancer Prev,* **14**, 4243-7.

Liu X, Tian W, Kolar B, et al (2011). MR diffusion tensor and perfusion-weighted imaging in preoperative grading of supratentorial nonenhancing gliomas. *Neuro Oncol*, **13**, 447-55.

Liu Z L, Zhou Q, Zeng Q S, et al (2012). Noninvasive evaluation of cerebral glioma grade by using diffusion-weighted imaging-guided single-voxel proton magnetic resonance spectroscopy. *J Int Med Res*, **40**, 76-84.

Lober R M, Cho Y J, Tang Y, et al (2014). Diffusion-weighted MRI derived apparent diffusion coefficient identifies prognostically distinct subgroups of pediatric diffuse intrinsic pontine glioma. *J Neurooncol*, **117**, 175-82.

Narasimhaiah D, Miquel C, Verhamme E, et al (2012). IDH1 mutation, a genetic alteration associated with adult gliomatosis cerebri. *Neuropathology*, **32**, 30-7.

Park S, Suh YL, Nam D H, et a1 (2009). Gliomatosis cerebri: clinicopathologic study of 33 cases and comparison of mass forming and diffuse types. *Clin Neuropathol*, **28**, 73-82.

Paulus W, Kleihues P (2010). Genetic profiling of CNS tumors extends histological classification. *Acta Neuropathol*, **120**, 269-70.

Porter K R, McCarthy B J, Freels S, et al (2010). Prevalence estimates for primary brain tumors in the United States by age, gender, behavior, and histology. *Neuro Oncol*, **12**, 520-7.

Romeike BFM, Mawrin C (2008). Gliomatosis cerebri: growing evidence for diffuse gliomas with wide invasion. *Expert Rev Neurother*, **8**, 587-97.

Rooney A G, McNamara S, Mackinnon M, et al (2013). Screening for major depressive disorder in adults with cerebral glioma: an initial validation of 3 self-report instruments. *Neuro Oncol*, **15**, 122-9.

RudàR, Bertero L, Sanson M (2014). Gliomatosis cerebri: A review. *Curr Treat Options Neurol,* 16, 1-9.

Rees JH (2011). Diagnosis and treatment in neuro-oncology: an oncological perspective. *Br J Radiol*, **2**, S82-9.

Sinha S, Bastin ME, Whittle IR, et al (2002). Diffusion tensor MR imaging of high-grade Gliomatosis cerebris. *Am J Neuroradiol*, **23**, 520-7.

Sun X, Vengoechea J, Elston R, et al (2012). A variable age of onset segregation model for linkage analysis, with correction for ascertainment, applied to glioma. *Cancer Epidemiol Biomarkers Prev*, **21**, 2242-51.

Taillibert S, Chodkiewicz C, Laigle-Donadey F, et al (2006). Gliomatosis cerebri: a review of 296 cases from the ANOCEF database and the literature. *J Neurooncol*, **76**, 201-5.

Zeybek U, Yaylim I, Ozkan NE, et al (2013). Cyclin D1 gene G870A variants and primary brain tumors. *Asian Pac J Cancer Prev,* **14**, 4101-6.

Zhang YB, Zhao W, Zeng RX (2013). Autophagic degradation of caspase-8 protects U87MG cells against H2O2-induced oxidative stress. *Asian Pac J Cancer Prev,* **14**, 4095-9.